Journal of Alloys and Compounds xxx (2008) xxx–xxx

Contents lists available at ScienceDirect

Journal of Alloys and Compounds

journal homepage: www.elsevier.com/locate/jallcom

Synthesis and luminescence properties of microemulsion-derived $Y_3Al_5O_{12}$: Eu^{3+} Phosphors

Chung-Hsin Lu [a,*], Chien-Hao Huang [a], Bing-Ming Cheng [b]

[a] Electronic and Electro-optical Ceramics Lab, Department of Chemical Engineering, National Taiwan University, Taipei, Taiwan, ROC
[b] National Synchrotron Radiation Research Center, Hsinchu, Taiwan, ROC

ARTICLE INFO

Article history:
Received 11 December 2007
Received in revised form 21 May 2008
Accepted 25 May 2008
Available online xxx

Keywords:
Microemulsion
Phosphors
Synthesis
Garnet

ABSTRACT

Europium-ion doped yttrium aluminum garnet (YAG: Eu^{3+}) phosphors were prepared via both the solid-state-reaction method and the microemulsion process. The solid-state-reaction-derived powders required repeated calcination at 1600 °C to produce phase-pure YAG: Eu^{3+}, and the formed phosphors had irregular morphology and a broad particle-size distribution. The microemulsion route was demonstrated to significantly lower the synthesis temperature of pure garnet phase to 1400 °C, and substantially reduce the particle size to submicron order. With a rise in the calcination temperature, the peak intensities in the excitation and emission spectra also increased as a result of increased amount of YAG phase. Synchrotron radiation-excited luminescence studies indicate that YAG: Eu^{3+} exhibited broad excitation peaks in vacuum ultraviolet (VUV) range and strong red emission peaks at 590 nm. The VUV-excited emission spectra demonstrate that the microemulsion-derived YAG: Eu^{3+} phosphors generated more intense luminescence than the solid-state-derived specimens. The enhanced luminescence characteristics are considered to be attributed to the reduced particle size and improved morphology of the microemulsion-derived phosphors.

1. Introduction

Ever since the introduction of tricolor fluorescent lamps using rare-earth ion-doped phosphors, research on luminescence applications is focused on the development of new types of phosphors. Newly launched devices such as plasma display panels (PDP) and field emission displays (FED) have attracted much attention because of their thinness, high brightness and superior picture quality. For improving the performance of displays, developing high-quality phosphors is a must. Besides the luminescence yield, the particle size, density, and morphology of phosphors also have to be well controlled [1–6]. The requirement that efficient phosphors utilize discharged inert gas as an excitation source has motivated vacuum ultraviolet (VUV) excited luminescence studies. When excited at 147 nm by discharged Xe gas, few phosphors have shown the potential for plasma display panels applications [1]. The phosphors used in PDP include $BaMgAl_{10}O_{17}$: Eu^{2+} and Y_2SiO_5: Ce^{3+} for blue emission, $BaAl_{12}O_{19}$: Mn^{2+} and Zn_2SiO_4: Mn^{2+} for green emission, and YBO_3: Eu^{3+} for red emission [7–12]. In most of the earlier reports, UV-light sources have been used to analyze the luminescence properties of the phosphors; however, rare studies have involved observations on VUV-excited emission.

Yttrium aluminum garnet ($Y_3Al_5O_{12}$, YAG) is an important material used for different kinds of electronic devices. Among the lanthanide-doped YAG materials, europium-ion-doped phosphors are regarded as potential red phosphors for applications in various luminescent devices. The luminescence properties of YAG: Eu^{3+} have been reported in crystals and ceramics prepared via the solid-state route [13,14]. However, phosphors prepared via the solid-state route usually have irregular morphology, large particles and wide particle size distributions. In order to reduce the particle size and improve the morphology of the prepared YAG: Eu^{3+} phosphors, a microemulsion process was adopted in this study. The reaction routes of microemulsion-derived YAG: Eu^{3+} were investigated and compared with those of the solid-state-reaction-derived phosphors. The prepared phosphors were investigated under high-energetic VUV excitation using synchrotron radiation as a light source. The effects of the preparation conditions on the VUV excited luminescence of the phosphors were also studied.

* Corresponding author at: Electronic and Electro-optical Ceramics Lab, Department of Chemical Engineering, National Taiwan University, No. 1, Sec. 4, Roosevelt Road, Taipei 106, Taiwan, ROC.
E-mail address: chlu@ntu.edu.tw (C.-H. Lu).

0925-8388/$ – see front matter © 2008 Elsevier B.V. All rights reserved.
doi:10.1016/j.jallcom.2008.05.081

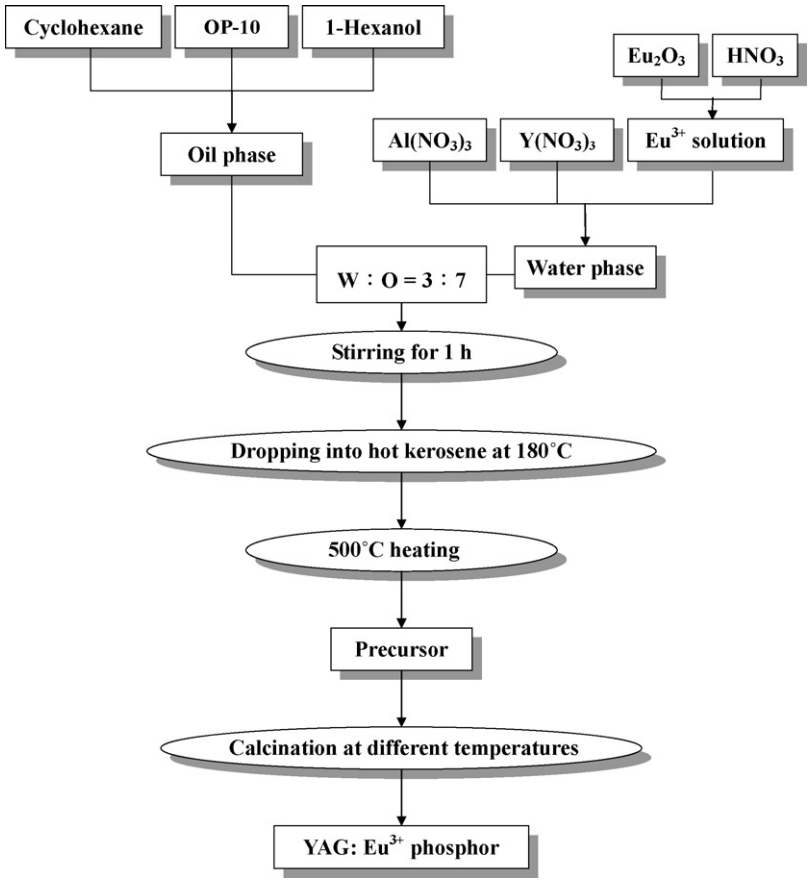

Fig. 1. Flowchart of the microemulsion process for synthesizing YAG: Eu^{3+} phosphors.

2. Experimental

2.1. Synthesis of YAG: Eu^{3+} phosphors

Yttrium oxide, aluminum oxide and europium oxide were mixed stoichiometrically according to the chemical formula $(Y_{0.95}Eu_{0.05})_3Al_5O_{12}$. The mixtures were ball-milled using zirconia (ZrO_2) balls with ethyl alcohol as the dispersing agent for 96 h. The slurry was subsequently dried in a vacuum-rotator dryer. The dried precursors were calcined at 800–1500 °C for 4 h, and then at 1600 °C for 4 h, before being ground again. The calcination and grinding processes were repeated for three times. The samples calcined at 1600 °C for three times is denoted SS-16.

Fig. 1 depicts the microemulsion process employed in this study for preparing YAG: Eu^{3+} phosphors. The microemulsion system was prepared in a mixture of water and oil with a water-to-oil (W/O) volume ratio of 3/7. Cyclohexane was chosen as the oil phase, and octylphenyl ether (OP-10) and 1-hexanol were used as the surfactant and co-surfactant, respectively. The amounts of cyclohexane, OP-10 and 1-hexanol were fixed at 50, 20, and 30 vol% of the total volume of the oil phase. The aqueous phase was prepared by dissolving appropriate amounts of yttrium nitrate, aluminum nitrate, and europium oxide in de-ionized water. The concentrations of yttrium ions, europium ions and aluminum ions in the solution were set to 0.285, 0.015, and 0.5 M, respectively. The cationic solutions were mixed according to the composition of $(Y_{0.95}Eu_{0.05})_3Al_5O_{12}$. After the prepared aqueous phase was mixed with the oil phase, the mixed solution was agitated for 1 h using a homogenizer to yield the well-emulsified solution, which was slowly dropped into 180 °C hot kerosene to evaporate water in the microemulsion. The obtained gels were dried at 500 °C for 2 h in air to remove the residual oil and obtain the precursor powders. The precursor powders were then ground and further calcined at various elevated temperatures ranging from 900 to 1400 °C for 4 h. The samples calcined at 1000, 1200, and 1400 °C are denoted EM-10, EM-12, and EM-14, respectively.

2.2. Characterization of YAG: Eu^{3+} phosphors

The phase purity and crystallinity of the powders were analyzed using an X-ray diffractometer (XRD, MAC science MXP3) with Cu Kα radiation. The morphology and particle sizes of the powders were examined using a scanning electron microscope (SEM, Hitachi S-800). The photoluminescence performance of the phosphor was recorded using a fluorescence spectrophotometer (Hitachi, F-4500) at room temperature. The luminescence characteristics of YAG: Eu^{3+} phosphors in the vacuum ultraviolet radiation range were investigated using synchrotron radiation at beam line BL03A at the National Synchrotron Radiation Research Center, Hsinchu, Taiwan. The VUV light produced in the center was dispersed with a high-flux cylindrical grating monochromator. The intensity of this VUV light was monitored by means of light reflected from a LiF beam splitter. A small fraction of the reflected beam passed through one additional LiF plate and was incident on a glass window coated with sodium salicylate. The fluorescence signal was detected by a photomultiplier tube in a photon-counting mode.

3. Results and discussion

3.1. Reaction routes of solid-state-reaction-derived YAG: Eu^{3+} phosphors

Fig. 2 shows the X-ray diffraction patterns of the solid-state-reaction-derived YAG: Eu^{3+} powders calcined under various conditions. After calcination at 800 °C, all detected peaks corresponded to Y_2O_3 and Al_2O_3 (Fig. 2(I)). After heating at 1000 °C, the reaction between Y_2O_3 and Al_2O_3 began to occur, and monoclinic $Y_4Al_2O_9$ (YAM) [15] formed along with a small amount of orthorhombic $YAlO_3$ [16] and hexagonal $YAlO_3$ (YAP) [17] (Fig. 2(II)). When the precursor powders were heated at 1200 °C, the YAM phase disappeared, along with an increase in the intensity of orthorhombic YAP peaks and a decrease in the intensity of hexagonal YAP peaks (Fig. 2(III)). When the heating temperature was elevated to 1400, 1500 and 1600 °C, $Y_3Al_5O_{12}$ appeared as the dominant phase; however, several peaks of orthorhombic YAP were still present (Fig. 2(IV)–(VI)). It is revealed that pure YAG: Eu^{3+} is difficult to obtain via the solid-state reaction. In order to obtain single-phased YAG: Eu^{3+}, the grinding and calcination processes at 1600 °C for 4 h were performed for three times. After the calci-

Please cite this article in press as: C.-H. Lu, et al., J. Alloys Compd. (2008), doi:10.1016/j.jallcom.2008.05.081

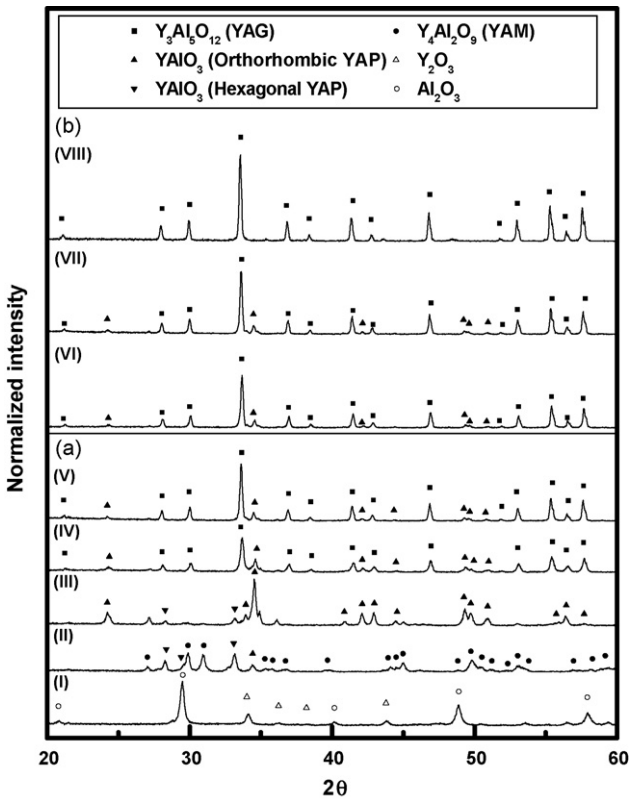

Fig. 2. X-ray diffraction patterns of YAG: Eu^{3+} phosphors prepared via the solid-state reaction method followed by (a) calcination at (I) 800 °C, (II) 1000 °C, (III) 1200 °C, (IV) 1400 °C and (V) 1500 °C for 4 h, and (b) repeated grinding and heating at 1600 °C for (VI) one time, (VII) two times, and (VIII) three times for 4 h.

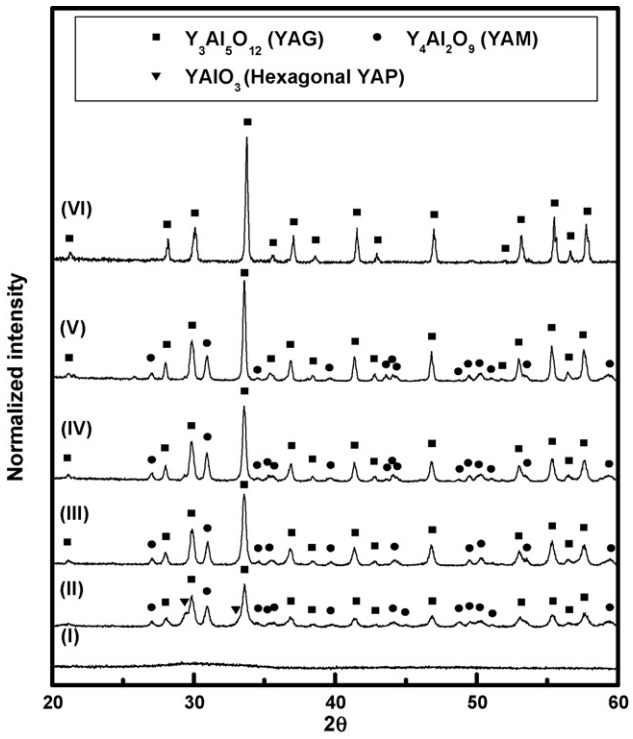

Fig. 3. X-ray diffraction patterns of YAG: Eu^{3+} phosphors prepared via the microemulsion process followed by calcination at (I) 500 °C, (II) 1000 °C, (III) 1100 °C, (IV) 1200 °C, (V) 1300 °C and (VI) 1400 °C in air for 4 h.

nation process was performed at 1600 °C for the second time, the amount of orthorhombic YAP significantly decreased (Fig. 2(VII)). As the calcination process was carried out at 1600 °C for three times, orthorhombic YAP completely disappeared and pure YAG: Eu^{3+} phosphors were obtained as shown in Fig. 2(VIII), with the evidence that the recorded XRD pattern of pure YAG: Eu^{3+} powders matched well with the standard powder diffraction file of YAG in the ICDD database (No. 33-0040) [18].

3.2. Reaction routes and morphology of the microemulsion-derived YAG: Eu^{3+} phosphors

Fig. 3 illustrates the X-ray diffraction patterns of the microemulsion-derived YAG: Eu^{3+} precursors calcined at various temperatures. For the sample calcined at 500 °C as shown in Fig. 3(I), no characteristic XRD peak was observed implying the absence of crystallized phase. After calcination at 1000 °C, YAG began to form with the coexistence of monoclinic YAM and hexagonal YAP (Fig. 3(II)). For the 1100 °C-calcined sample, hexagonal YAP disappeared, and YAG coexisted with YAM. With a further increase in the heating temperature, the amount of YAM decreased along with an increase in the amount of YAG. When the heating temperature reached 1400 °C, pure YAG phase was successfully obtained.

It was found that the main intermediate compounds formed in the microemulsion-derived precursors and solid-state-reaction-derived precursors were YAM and YAP. In addition, the microemulsion-derived precursors yielded phase-pure YAG after calcination at 1400 °C, which is 200 °C lower than that required in the solid-state-reaction process. The lowering of the formation temperature of pure YAG is considered to be attributed to the enhanced homogeneity of constituent species and increased reactivity in the microemulsion-derived precursors. In comparison with the sol–gel process [19], the microemulsion process needs to increase the heating temperatures for obtaining the pure compound. Heating at elevated temperatures results in improvement in crystallinity.

Fig. 4(a)–(c) shows the morphology of YAG: Eu^{3+} precursors prepared via the microemulsion process followed by calcination at various temperatures. The formed powders mainly comprised spherical and uniformly submicron-sized particles. As the calcination temperature was raised from 1000 to 1400 °C, the average particle size enlarged from 100 to around 300 nm (see Fig. 4(a) and (c)). On the other hand, the powders obtained via the solid-state reaction exhibited irregular morphology and large particles size (around 1–3 μm) as shown in Fig. 4(d). It is revealed that the microemulsion process effectively led to reduced particle size and improved morphology of YAG: Eu^{3+} powders. The coarsening and agglomeration of grains occurring in the solid-state reaction was a result of high-temperature calcination and prolonged heating.

3.3. UV-excited luminescence characteristics of microemulsion-derived YAG: Eu^{3+} phosphors

Fig. 5 illustrates the photoluminescence excitation spectra of the microemulsion-derived YAG: Eu^{3+} precursors calcined at various temperatures. Monitoring at 590 nm yielded a band with a maximum at 238 nm for the sample calcined at 1000 °C (EM-10) as depicted in Fig. 5(a). This band was attributed to the presence of the YAG phase and the appearance of the excitation spectra confirmed the entrance of Eu^{3+} ions into the crystallographic sites of YAG. When the calcination temperatures were raised to 1200 and 1400 °C, similar excitation spectra were observed for samples EM-12 and EM-14 as illustrated in Fig. 5(b) and (c). However, the intensities of the peaks in the excitation spectra increased with heating temperature due to the increase in the amount of YAG phase

Please cite this article in press as: C.-H. Lu, et al., J. Alloys Compd. (2008), doi:10.1016/j.jallcom.2008.05.081

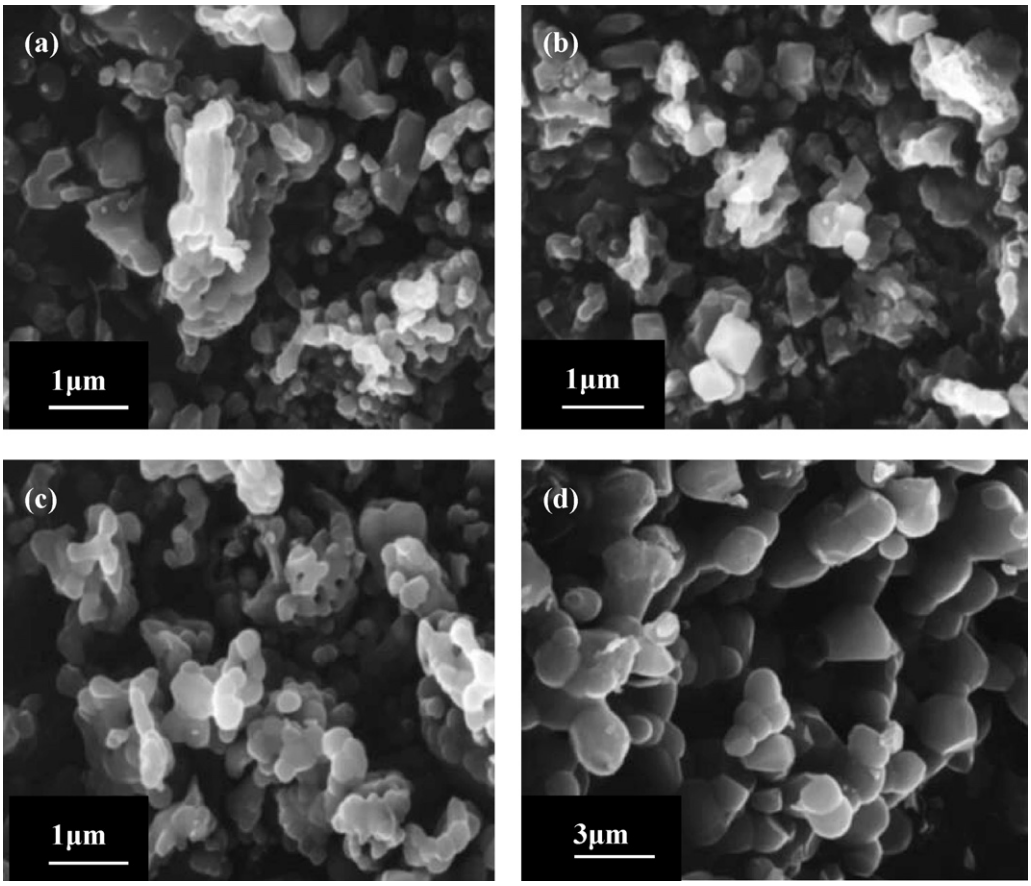

Fig. 4. SEM photographs of the microemulsion-derived YAG: Eu^{3+} phosphors with calcination at (a) 1000 °C, (b) 1200 °C and (c) 1400 °C for 4 h, and (d) the solid-state-derived YAG: Eu^{3+} phosphors with calcination at 1600 °C for three times.

as shown in Fig. 3. The 395-nm peak in the excitation spectra is associated with the intra-configurational $4f^6$ transitions of Eu^{3+} ions [20]. In addition, the band observed in the region of 200–275 nm corresponds to the charge transfer band (CTB) of Eu^{3+}–O^{2-} [21].

Fig. 6 illustrates the emission spectra of microemulsion-derived YAG: Eu^{3+} calcined at various temperatures. For the sample calcined at 1000 °C (EM-10) as shown in Fig. 6(a), the 238-nm excited spectrum reveals the coexistence of YAM: Eu^{3+} and YAG: Eu^{3+}. The main peaks at 590 and 613 nm correspond to the $^5D_0 \rightarrow {}^7F_1$ transition of Eu^{3+} in YAG and the $^5D_0 \rightarrow {}^7F_2$ transition of Eu^{3+} in YAM, respectively. For the sample calcined at 1200 °C (EM-12) as depicted in Fig. 6(b), the similar emission spectrum was observed; however, an increase in the intensity of the 590-nm peak and a decrease in the intensity of 613 nm peak were also found. This indicates that the amount of YAG was increased and the amount of YAM was correspondingly reduced. As the temperature was raised to 1400 °C (EM-14), only the spectrum belonging to YAG was observed and the intensities of the peaks were significantly increased. The dominant peak at 590 nm corresponds to the $^5D_0 \rightarrow {}^7F_1$ transition and the other peak at 608 nm is related to the $^5D_0 \rightarrow {}^7F_2$ transition [22].

The intensity of the transitions between different J levels depends on the symmetry of the local environment of the Eu^{3+} activators [23]. According to the transition selection rules $\Delta J = 0 \pm 1$ and $\Delta S = 0$, magnetic dipole transition ($^5D_0 \rightarrow {}^7F_1$) is allowed, and electric dipole transition ($^5D_0 \rightarrow {}^7F_2$) is forbidden. However, in some cases in which Eu^{3+} activators occupy sites without inversion symmetry, the parity forbiddance is not strictly maintained and the spectra resulting from the electric dipole transition appear.

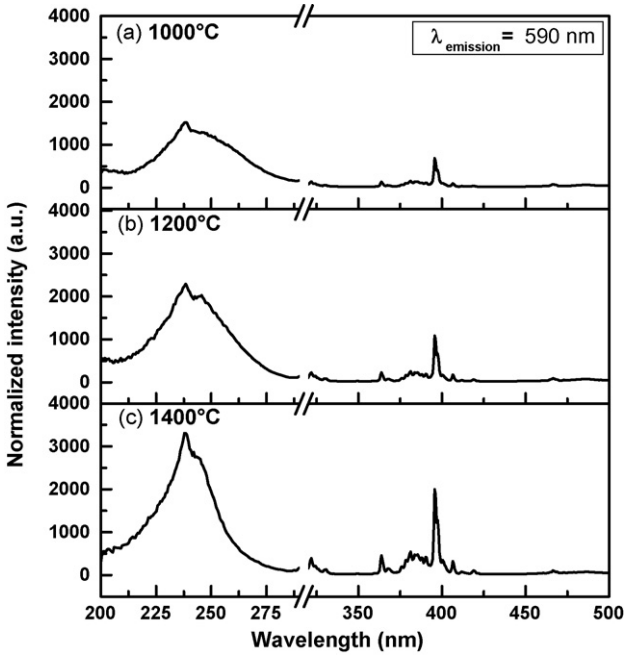

Fig. 5. Photoluminescence excitation spectra monitored at $\lambda_{emission}$ = 590 nm for the microemulsion-derived YAG: Eu^{3+} phosphors calcined at various temperatures.

Please cite this article in press as: C.-H. Lu, et al., J. Alloys Compd. (2008), doi:10.1016/j.jallcom.2008.05.081

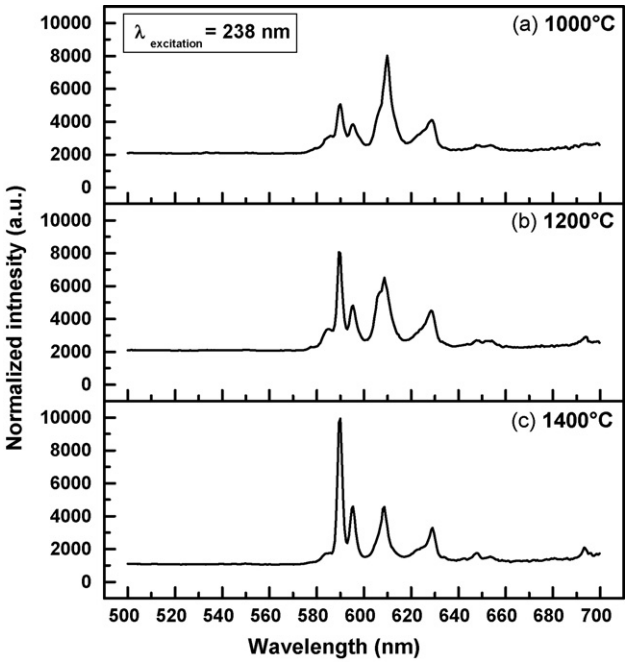

Fig. 6. Photoluminescence emission spectra upon excitation at 238 nm for the microemulsion-derived YAG: Eu^{3+} phosphors calcined at various temperatures.

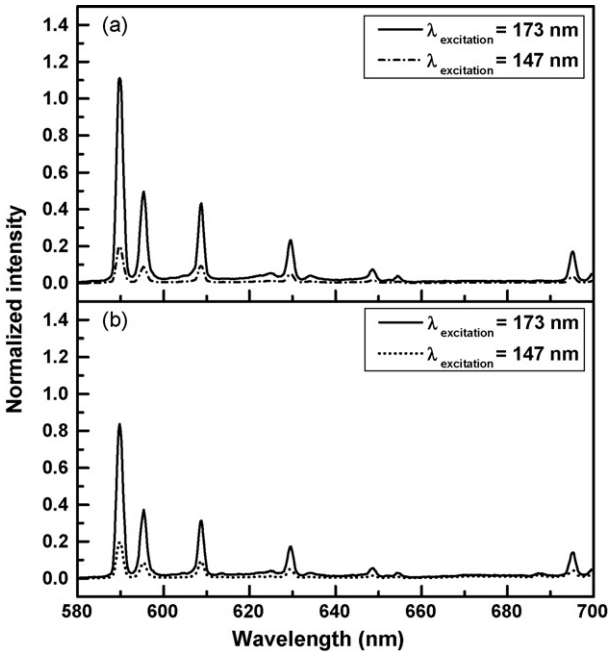

Fig. 8. Photoluminescence emission spectra of YAG: Eu^{3+} phosphors (a) EM-14 and (b) SS-16, upon VUV-light excitation and recorded via a synchrotron radiation facility.

3.4. VUV-excited luminescence characteristics of the solid-state-reaction-derived and microemulsion-derived YAG: Eu^{3+} phosphors

The excitation spectra in the VUV region monitored at 590 nm were recorded for YAG: Eu^{3+} phosphors prepared via the solid-state reaction (SS-16) and microemulsion route (EM-14). Similar excitation characteristics are observed in Fig. 7. The excitation spectra result from the $4f^{n-1}$–5d transition of Eu^{3+}, host absorption, excitonic transition and charge transfer. The band gap of YAG is reported to be 6.5 eV (190 nm) [23]. Taking into consideration of the energy of the onset of host absorption, the excitation spectra can be divided into two regions: (i) charge transfer absorption above 190 nm, and (ii) fundamental absorption below 190 nm. However, the relative intensities of these two regions reveal a considerably large difference between the samples prepared via these two methods. The excitation spectrum of the microemulsion-derived YAG: Eu^{3+} reveals a strong absorption in the fundamental absorption region. During the solid-state reactions, grinding processes were repeated for several times. Defects were formed on the surface of powders during grinding. It is considered that formed defects in the solid-state-derived powders cause to reduce the fundamental absorption.

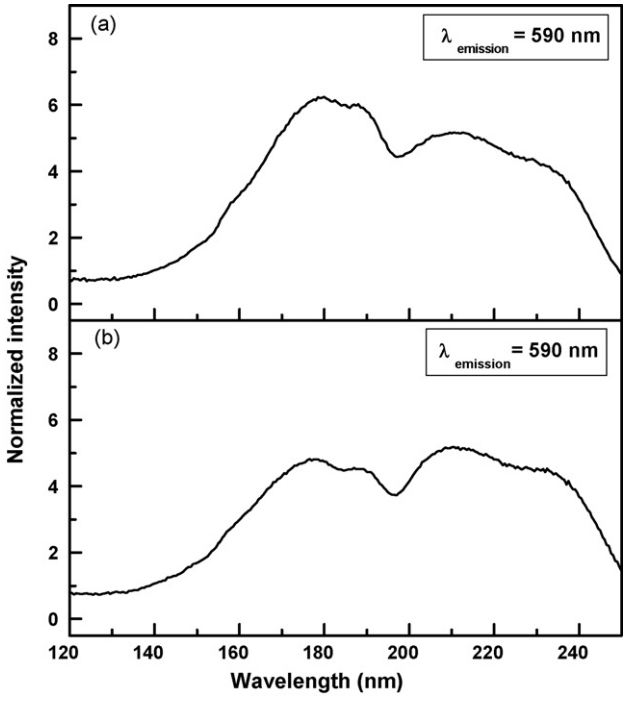

Fig. 7. Photoluminescence excitation spectra of YAG: Eu^{3+} phosphors (a) EM-14 and (b) SS-16, monitored at $\lambda_{emission}$ = 590 nm and recorded via a synchrotron radiation facility.

Fig. 8 shows the emission spectra of YAG: Eu^{3+} phosphors synthesized via the two processes, under excitation at 147 and 173 nm with VUV light. Similar emission spectra in the 580 to 700 nm region are observed for powders prepared via both processes. The major emission peak near 590 nm is attributed to the $^5D_0 \rightarrow {}^7F_1$ magnetic dipole transition of Eu^{3+} ions, while the minor peaks at 608 nm is assigned to $^5D_0 \rightarrow {}^7F_2$ electric dipole transitions [21]. The intensity ratio ($R = I_{608}/I_{590}$) between $^5D_0 \rightarrow {}^7F_2$ (at 608 nm) and $^5D_0 \rightarrow {}^7F_1$ (at 590 nm) transitions can be used to evaluate the site symmetry for Eu^{3+}. [23] It was found that the microemulsion-derived powders had a larger R value ($R = 3.9$) than the solid-state-derived powders ($R = 3.7$), suggesting greater distortion of the local environment of Eu^{3+} ions in microemulsion-derived YAG. The probability of $^5D_0 \rightarrow {}^7F_2$ transition is increased as a result of this distortion. The emission intensity of the microemulsion-derived phosphors was found to be higher than that of the solid-state-derived phosphors. It is attributed to the decreased particle size and improved morphology of the microemulsion-derived powders. In the solid-state reaction, the prolonged heating promotes agglomeration and coarsening of grains, and repeated

Please cite this article in press as: C.-H. Lu, et al., J. Alloys Compd. (2008), doi:10.1016/j.jallcom.2008.05.081

grinding produces defects on the surface of the phosphors, thereby increasing non-radiative relaxations and causing a decrease in the emission efficiency. Conclusively, the microemulsion process was confirmed to be a potential method to prepare YAG: Eu^{3+} phosphors with improved photoluminescence properties.

4. Conclusions

$Y_3Al_5O_{12}$: Eu^{3+} (YAG: Eu^{3+}) phosphors were prepared via both the solid-state reaction and microemulsion process. The solid-state reaction required high-temperature heating to prepare pure garnet phase, and the formed particles exhibited irregular morphology with a broad particle-size distribution. On the other hand, the microemulsion route effectively lowered the synthesis temperature of pure garnet phase to 1400 °C and reduced the particle size to submicron order. The intensities of the peaks in the excitation and emission spectra markedly increased with the calcination temperature owing to an increase in the amount of YAG phase. According to the results of the synchrotron radiation-excited luminescence studies, it is confirmed that YAG: Eu^{3+} exhibited broad excitation peaks in VUV range and strong red emission peaks at 590 nm. In addition, the microemulsion-derived YAG: Eu^{3+} phosphors were found to generate more intense luminescence than the solid-state-derived powders. The reduced particle size and improved morphology in the microemulsion-derived phosphors are regarded as the factors for enhancing the luminescence characteristics.

Acknowledgement

The authors would like to thank Mr. Hong-Kai Chen and Miss Hsiao-Chi Lu at the National Synchrotron Radiation Research Center, Taiwan for their help in measuring the VUV excitation spectra.

References

[1] K. Nonomura, H. Higashino, R. Murai, Mater. Res. Bull. 11 (2002) 898.
[2] X. Zhang, Q. Li, Y. Tu, Y. Tang, J. Xia, Y. Zheng, B. Wang, H. Yin, L. Tong, SID 02 Digest 33 (2002) 748.
[3] Y.C. Kang, I.W. Lenggoro, S.B. Park, K. Okuyama, Mater. Res. Bull. 35 (2000) 789.
[4] K. Betsui, F. Namiki, Y. Kanazawa, H. Inoue, Fujitsu Sci. Tech. J. 35 (1999) 229.
[5] K. Yoshikawa, Y. Kanazawa, M. Wakitani, T. Shinoda, A. Otsuka, Tech. Rep. Inst. TV Eng. Jpn. 16 (1992) 17.
[6] J. Koike, T. Kojima, R. Toyonaga, A. Kagami, T. Hase, S. Inaho, J. Electrochem. Soc. 126 (1979) 1008.
[7] K.C. Mishra, M. Raukas, G. Marking, P. Chen, P. Boolchand, J. Electrochem. Soc. 152 (2005) H183.
[8] D.W. Cooke, J.K. Lee, B.L. Bennett, J.R. Groves, L.G. Jacobsohn, E.A. McKigney, Appl. Phys. Lett. 88 (2006) 103108.
[9] D.Y. Lee, Y.C. Kang, H.D. Park, S.K. Ryu, J. Alloy. Compd. 353 (2003) 252.
[10] P. Thiyagarajan, M. Kottaisamy, M.S. Ramachandra Rao, J. Electrochem. Soc. 154 (2007) H297.
[11] E.J. Popovici, L. Muresan, H. Amalia, E. Indrea, M. Vasilescu, J. Alloy. Compd. 434–435 (2007) 809.
[12] K.S. Sohn, I.W. Zeon, H. Chang, S.K. Lee, H.D. Park, Chem. Mater. 14 (2002) 2140.
[13] M. Sekita, H. Haneda, S. Shirasaki, T. Yanagitani, J. Appl. Phys. 69 (1991) 3709.
[14] J.A. Koningstein, Phys. Rev. 136 (1964) A717.
[15] Powder Diffraction File, Card No. 33-0041, Joint committee on powder diffraction standards, Swarthmore, PA.
[16] Powder Diffraction File, Card No. 34-0368, Joint committee on powder diffraction standards, Swarthmore, PA.
[17] Powder Diffraction File, Card No. 16-0219, Joint committee on powder diffraction standards, Swarthmore, PA.
[18] Powder Diffraction File, Card No. 33-0040, Joint committee on powder diffraction standards, Swarthmore, PA.
[19] C.H. Lu, W.T. Hsu, C.H. Hsu, H.C. Lu, B.M. Cheng, J. Alloys Compd. 456 (2008) 57.
[20] B.G. Wybourne, Spectroscopic properties of rare-earths, Interscience, New York, 1965.
[21] Y.H. Zhou, J. Lin, S.B. Wang, H.J. Zhang, Opt. Mater. 20 (2002) 13.
[22] D. Ravichandran, R. Roy, A.G. Chakhovskoi, C.E. Hunt, W.B. White, S. Erdei, J. Lumin. 71 (1997) 291.
[23] C.W. Thiel, H. Cruguel, Y. Sun, G.J. Lapeyre, R.M. Macfarlane, R.W. Equall, R.L. Cone, J. Lumin. 94 (2001) 1.